

THE INTEGRATION OF REMOTE SENSED IMAGES AND DTM DATA

Weihsin Ho
 Department of civil engineering
 National Chiao Tung University
 1001 Ta-shuei Rd. Hsinchu Taiwan, R.O.C.

Liang Huei Lee
 Department of surveying and mapping
 Chung Cheng Institute of Technology
 Ta-hsi Toayuang Taiwan, R.O.C.

ABSTRACT

Images obtained from remote sensors and information of DTM are the important data sources for GIS. Especially, three dimensional image-based display has better visualization effect than three dimensional vector-based one. The integrated usage of these two kinds of information is the important direction of development in GIS. In this paper, we will discuss the processing of integration of remote sensed images and DTM data. The topics include (a) to capture image-based terrain features which can be displayed alone or with remote sensed images together, (b) to do 3D projections of remote sensed images for landscape visualization, and (c) to simulate a stereopair from a single image. The principle of processing is to satisfy the condition of that each pixel on images should match with a certain height within DTM. The resolution of these two kinds of data is different, therefore in general, the DTM data should be processed by interpolation to subject to those of images. In the paper, we also propose the algorithms for different situations such as terrain slope, aspect, ridge lines, valleys, streams and shadows etc.

Keyword: GIS, DTM, landscape visualization

I. INTRODUCTION

GIS is a information system of spatial data. It is widely applied to the related realms of resource management and planning [15]. In GIS, a lot of land surface information is obtained from remote sensed images and DTM data. Furthermore, images is also the important data source when spatial data is updated. At the present time, many GIS are vector-based systems. Hence, the display is vector linework in such systems. However, linework display has worse visualization effect than raster-based image display. And there is a lot of information of the terrain features that can be derived from raster images. Therefore, how to combine these two kinds of information is one of the important trends in GIS community. There are many applications which need the integrated information of remote sensed images and DTM data. Basically, remote sensed images can be processed with DTM data in the followings: (1) ortho-rectification for the registration with map coordinates, (2) raster-based extraction of terrain features, (3) the 3D projective transformation, and (4) simulated stereopair from a single frame of images. The principle of processing is to content that each pixel on images should match with a certain height within DTM. The resolution of these two kinds of data is different, so in general, the DTM data should be processed by interpolation to coincide with those of images. In this paper, we introduce some preprocessing of DTM data first. We also propose the algorithms for different situations such as the extraction of terrain slope, shadows etc. Finally, 3D transformation models and stereopair simulation have processed by means of methods of computational vision.

II. DTM DATA PROCESSING

2-1 FILTERING

DTM data obtained from profile scanning or image correlation method contains dynamic scanning noise and measurement errors. This process is a smoothing procedure to reduce noise and error. We can delineate the dynamic scanning using the following differential equations [1]:

$$Z^* = Z + r_1 Z + r_2 \ddot{Z} \tag{1}$$

$$\dot{Z} = \frac{dz}{dy} = \frac{Z_{i+1} - Z_{i-1}}{2 \Delta y} \tag{2}$$

$$\ddot{Z} = \frac{d^2z}{dy^2} = \frac{Z_{i+1} - 2Z_i + Z_{i-1}}{\Delta y^2} \tag{3}$$

where Δy is DTM interval which can be normalized to 1,

r_1, r_2 are filtering parameters, and Z^*, Z are real height and measured height respectively.

Because real height, Z^* is difficult to obtain, it can be replaced by the height from the neighboring profiles with self-calibration filtering, i.e.

$$Z - Z^* = \frac{2Z_{j,i} - Z_{j-1,i} - Z_{j+1,i}}{4} \tag{4}$$

where j is a number of profiles ($j=1,2,\dots,m$), and i is a resampling point in the j th profile. Combining eq.(1) to eq.(4), we can solve the filtering parameters using the least squares method based on 3 to 5 profiles. Then the height after filtering can be calculated with respect to the parameters.

2-2 GRID INTERPOLATION WITH SLOPE-CONSTRAINED CONDITION

The sampling interval of grid DTM data is larger than image resolution. For the integrated usage of these two kinds of data, in general, the DTM data should be processed by interpolation to match the resolution of images. The interpolation is implemented with 4x4 cubic convolution [12]. The matrix formula is as follow:

$$Z_p = \begin{bmatrix} f_4(t) \\ f_3(t) \\ f_2(t) \\ f_1(t) \end{bmatrix}^T \begin{bmatrix} Z_{11} & Z_{12} & Z_{13} & Z_{14} \\ Z_{21} & Z_{22} & Z_{23} & Z_{24} \\ Z_{31} & Z_{32} & Z_{33} & Z_{34} \\ Z_{41} & Z_{42} & Z_{43} & Z_{44} \end{bmatrix} \begin{bmatrix} f_1(t) \\ f_2(t) \\ f_3(t) \\ f_4(t) \end{bmatrix} \quad (5)$$

where Z_{ij} is grid height in Fig. 1, and Z_p is desired height. If it is supposed that the surface passes through all of 4x4 grid, $f_k(t)$ can be described as :

$$\begin{aligned} f_1(t) &= -\frac{1}{6}t^3 + \frac{1}{2}t^2 - \frac{1}{3}t \\ f_2(t) &= \frac{1}{2}t^3 - t^2 + \frac{1}{2}t + 1 \\ f_3(t) &= -\frac{1}{2}t^3 + \frac{1}{2}t^2 + t \\ f_4(t) &= \frac{1}{6}t^3 - \frac{1}{6}t + \frac{10}{3} \end{aligned} \quad (6a)$$

Where t is the x, y coordinates of normalized interpolated point p , i.e. $0 < t < 1$. If the surface only passes through the central four points of grid, this four points will be constrained by slope condition. For example, Z_{12} is the height of point (12) and its slope is $(Z_{13} - Z_{12})/2$. The height of point (13) is Z and its slope is $(Z_{14} - Z_{12})/2$. Then $f(t)$ can be modified as follow:

$$\begin{aligned} f_1(t) &= -\frac{1}{2}t^3 + t^2 - \frac{1}{2}t \\ f_2(t) &= \frac{3}{2}t^3 - \frac{5}{2}t^2 + 1 \\ f_3(t) &= -\frac{3}{2}t^3 + 2t^2 + \frac{1}{2}t \\ f_4(t) &= \frac{1}{2}t^3 - \frac{1}{2}t \end{aligned} \quad (6b)$$

2-3 GRID INTERPOLATION WITH RANDOM DISCRETE POINTS

For the convenience of editing, this approach is designed as following two different algorithms.

2-3-1 TIN STRUCTURE

A triangulated irregular network (TIN) is established from the all random sampling points according to Delaunay triangulated network [10]. Then each triangle has been processed as a regular grid by interpolation. Figure 2 is the principle of interpolation. The primary advantage is that the break line or feature line of terrain can be easily portrayed by this method. However, the surface structured by TIN has worse feasibility and precision except sampling density is adequate. The flowchart of processing procedures is diagramed in Figure 3.

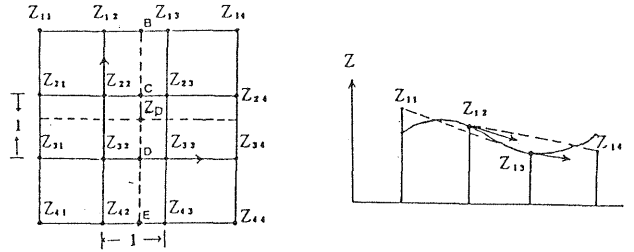


Figure 1 Increasing the density of DTM by interpolation

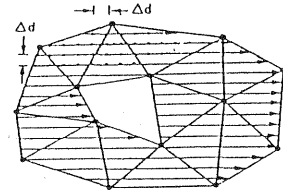


Figure 2 The principle of grid DTM from TIN

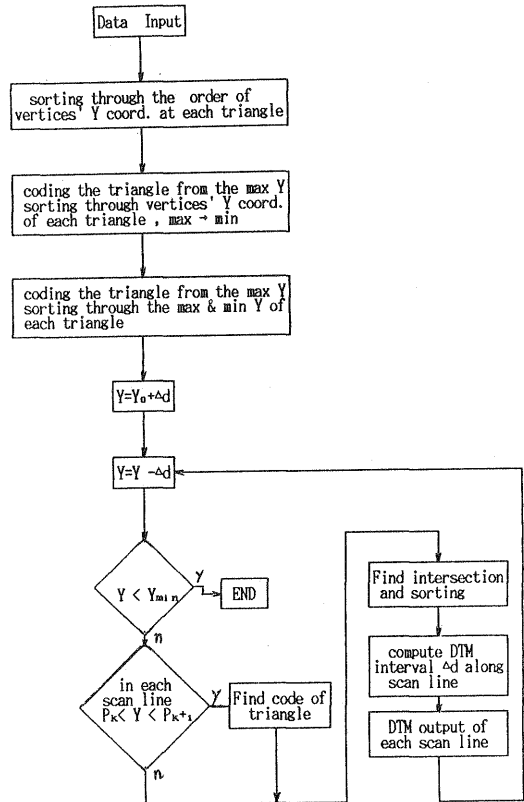


Figure 3 The procedures of DTM generation from TIN

2-3-2 INTERPOLATION WITH POINT BY POINT

It is necessary to select new reference points while a point is inserted by this method. The principle of this method is shown in Figure 4. At the first, we define the effective area for DTM sampling that means what area will be sampled or not. For deciding the interval of interpolation, all intersections of each scan line and defined area should be determined, before interpolation is processing. As mentioned above, there are N reference points to be selected in neighborhood of sampling point. Then suitable interpolation model is used according to accuracy criterion, e.g. weighted moving average method, bilinear interpolation, two-order polynomials and linear least squares prediction etc. Although the result of surface modelling is more feasible, description of terrain features is still worse due to grid DTM. And it is time-consuming especially as the number of reference points is increasing.

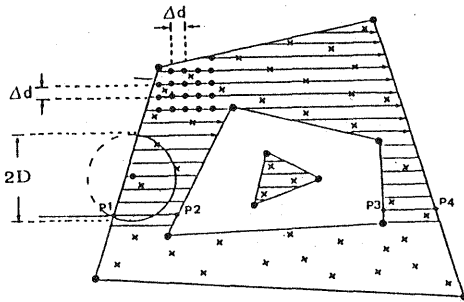


Figure 4 The principle of interpolation with point by point

2-4 CASE STUDY

The case study is based on a topographic map used for the design of a golf court. The shape of study area is irregular. There are total 514 random points in the area which is gained by digitizing contour lines. The Delaunay triangulated network for a set of 514 random points is shown in Figure 5. Figure 6 is the original contour map of the study area. The polygon of the area is constituted with 166 vertices. Then a 65x65 grid DTM is generated by the methods mentioned above, i.e. TIN and point by point methods. Heights outside the study area are given by negative values and are not processed. Fig. 7 shows the contour map which is the result of TIN method and Fig. 8 shows the result of point by point method with least squares prediction.

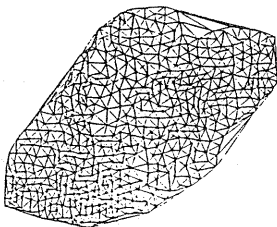


Figure 5 The Delaunay triangulated network for a set of 514 points

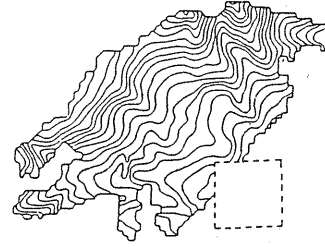


Figure 6 The original contour map of test area

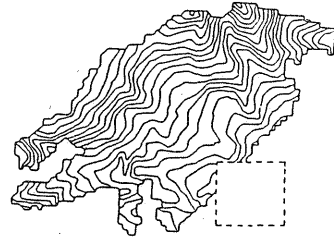


Figure 7 The contour map obtained from the result of TIN

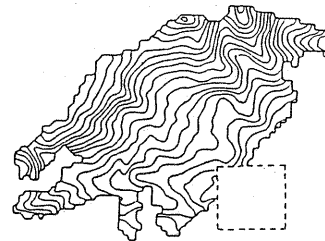


Figure 8 The contour map obtained from the result of point by point with least squares prediction method

III. EXTRACTION OF TERRAIN FEATURES FROM DTM

The extraction of terrain features from DTM can be done by either raster or vector methods. In fact, extracting terrain features and display the result by raster method is simpler than vector method. Moreover, raster display has better effect in landscape visualization. Slope gradient and aspect in each grid can be computed with DTM data[13]. Feature lines of terrain, such as ridges and valleys, are the important factors of describing the characteristics of terrain. They are helpful for interpretation of streams and watersheds and can be used as reference features for image matching [16, 3, 6]. For example, a 3x3 operating mask is used to decide ridges. If the central pixel P contents with following three criterions, then pixel P is a ridge:

1. Height of pixel P is not the lowest when it compare to heights of neighboring 8 points, see Figure 9.

2. Height of pixel P should be the highest on one of four profiles which pass through pixel P.
3. Pixel P is not a single pixel.

8	1	2
7	P	3
6	5	4

Figure 9 A 3x3 operating mask

The criterion 1 and 2 are opposite in extracting valleys. The shadow of terrain can be gained by hill shading method. The simulated sunshined images is produced by computing the density of reflection according to the difference of terrain releaf, incident light source and position of viewpoint. Therefore, before computation has been accomplished, the positions of sun light and viewpoint must be defined. The simulated sunshined images has geometry of ortho- projection and the appearance of terrain releaf is augmented by shadow to present a stereo effect [5]. This approach has been applied in computer assisted mapping and computer vision [18,2].

IV. THREE DIMENSIONAL IMAGES REPRESENTATION FOR COMPUTER VISION

Terrain surface has the property of random releaf and contains a plenty of information of features. The images from remote sensors presents only planar scenery and lacks a stereo vision effect. Three dimensional images display has effect of stereo vision and is completed through a transformation of mathematic projection using both remote sensed images and DTM data. This approach is called landscape visualization [8,11] and has been applied to many disciplines such as GIS, war game and flight simulation etc. In computer graphics, 3D images display is performed by 3D transformation using a homogeneous coordinate system [17]. This approach is also applied to landscape visualzition [7,13]. In this paper, we introduce the colinear equations which are well known in photogrammetry. The colinear equations are used to describe the relationship between object space and projective plane with computational vision method while the spatial position of viewpoint is given. This approach is convenient for the setup or simulation of conditional parameters of actual visualzition. In this section, we will illustrate the data preprocessing and related algorithms design.

4-1 THE PREPROCESSING OF IMAGES AND DTM DATA

The purpose of preprocessing is to make each pixel on images coincidence with a ground elevation. Therefore, the procedures include increasing DTM density by interpolation and ortho-rectification of images. If the MSS images from satellite is used, then color enhancement must be performed first. This enhancement can make images better color effect. We can derive the true color scene from RGB bands of LANDSAT TM images. However, it still presents the lacks of enough color saturation and causes lower hue although the

contrast enhancement has been done [4]. For overcoming this problem, the color coordinate transformation is used to achieve color enhancement [9].

4-2 TRANSFORMATION OF PARALLEL PROJECTION

The viewpoint is defined at infinite in parallel projection. Hence, the 3D coordintes of points in object space are sequently projected on 2D plane along the direction parallel to the sight line. The object coordinates (X_p, Y_p, Z_p) of object point P is transformed to the image coordinates (x_q, y_q) of projective point Q, i.e.

$$X_g = X_p \cos \alpha + Y_p \sin \alpha$$

$$Y_g = Z_p \cos \beta + (-X_p \sin \alpha + Y_p \cos \alpha - Z_p) \sin \beta \quad (7)$$

where α is the azimuth of sight line, and β is the roll of sight line.

4-3 TRANSFORMATION OF PERSPECTIVE PROJECTION

If the orientation parameters of perspective center (viewpoint) and the location of projective plane are decided, then the 3D coordinates of object can be projected on 2D plane. The formulas are well known in photogrammetry and written as:

$$X_g = -f \frac{a_{11}(X_p - X_0) + a_{12}(Y_p - Y_0) + a_{13}(Z_p - Z_0)}{a_{31}(X_p - X_0) + a_{32}(Y_p - Y_0) + a_{33}(Z_p - Z_0)}$$

$$Y_g = -f \frac{a_{21}(X_p - X_0) + a_{22}(Y_p - Y_0) + a_{23}(Z_p - Z_0)}{a_{31}(X_p - X_0) + a_{32}(Y_p - Y_0) + a_{33}(Z_p - Z_0)} \quad (8)$$

$$a_{11} = \cos \beta \cos \alpha$$

$$a_{12} = \cos \beta \sin \alpha$$

$$a_{13} = -\sin \beta$$

$$a_{21} = \sin \gamma \sin \beta \cos \alpha - \cos \gamma \sin \alpha$$

$$a_{22} = \sin \gamma \sin \beta \sin \alpha + \cos \gamma \cos \alpha \quad (9)$$

$$a_{23} = \sin \gamma \cos \beta$$

$$a_{31} = \cos \gamma \sin \beta \cos \alpha - \sin \gamma \sin \alpha$$

$$a_{32} = \cos \gamma \sin \beta \sin \alpha - \sin \gamma \cos \alpha$$

$$a_{33} = \cos \gamma \cos \beta$$

where α is the yaw of sight line,
 β is the pitch of sight line, and
 γ is the roll of sight line.

4-4 TRANSFORMATION OF PANORAMIC PROJECTION

Panoramic projection is similar as cylinder projection and the viewpoint O is located at the central axis of cylinder. Then the object point P is project on the plane of cylinder and the equations are written as:

$$x_q = \alpha_p r \quad (10)$$

$$y_q = Z_0 + \frac{r}{l_p} (Z_p - Z_0)$$

where α is the polar angle of object point P,
 l is the distance between object point and central axis of cylinder,
 z is the coordinate of cylinder system,
and r is the radius of cylinder.

4-5 ALGORITHM DESIGN

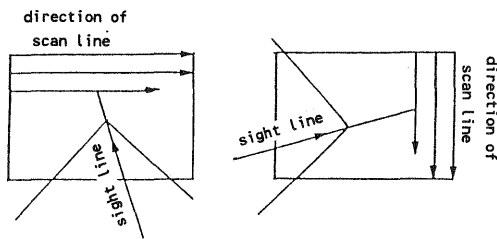
The purpose of projective transformation is to project the 3D coordinates on 2D display plane. In fact, because the terrain releaf is different in different place, there are many hidden points to be processed during the

transformation is performed. The processing of hidden point is an important subject in computer graphics. There are different algorithms for different types of data [17].

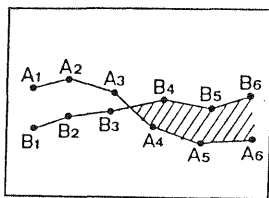
Although the algorithm that we will illustrate is worse in computation efficiency, there is smaller in memory requirement. It can handle a large volume of data. The procedures are as follows:

1. The images and DTM data are sorted based on the defined yaw of sight line and let the angle between scan line and sight line be greater than 45 shown as in Figure 10 (a).
2. Starting at the scan line which is farthest away from viewpoint, and the projected coordinates are computed and recorded, e.g. points A_i and B_i in Figure 10 (b).

Judgement: If the segment of A_i is over the segment of B_i , then it is in sight, else it is a hidden part. For example, the shading part is hidden in Figure 10 (b).



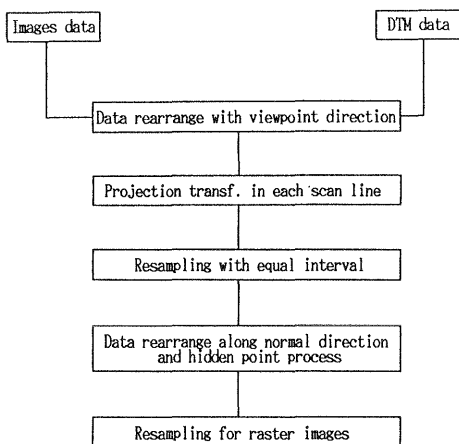
(a) Data is rearranged with respect to the direction of viewpoint



(b) The judgement of the part of hidden

Figure 10 The Procession of hidden points

The summary of procedures is diagramed as follows:



4-6 SIMULATION OF A STEREOPAIR IMAGES

Using a single frame of images and coincided DTM data, the x parallax can be simulated based on the difference of height releaf between pixels. Then the another new images can be obtained by resampling using the information of x parallax. This simulated images and original images constitute a stereopair. The principle of simulation is shown in Figure 11.

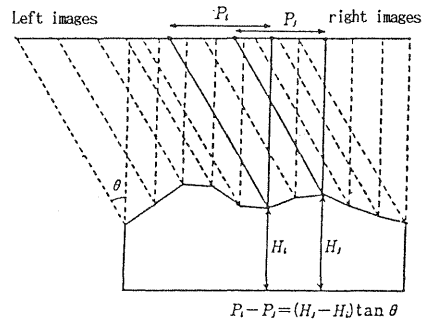


Figure 11 The simulation of a stereopair of images

V. EXAMPLES

The original DTM data used in all examples is 40m interval which is offered by the Institute of Photogrammetry, Forest Bureau, Taiwan. The images used is 512x512. After filtering procession, the terrain features are extracted such as terrain shading, contour, slope gradient and aspect, ridges and valleys etc. The results are shown as plates 1 to 8. In the examples of 3D images display, the LANDSAT TM images, located at the north of Taiwan, is used which was taken in 1986. The images has been processed by geometric rectification and color enhancement. Then the various 3D projective transformations and stereopair simulation were proceeded with DTM data. The results and original data are shown in plates 9 to 17. All processing were completed on PC/AT-386(33MHz). The perspective transformation took the longest time, e.g. the total execution time was two minutes and twenty seconds for 512x512 single band images.

VI. CONCLUSION

Basically, remote sensed images can provide the planar information of terrain and DTM data can supply the elevation information. Therefore, the integration of geometric rectified images with DTM data can furnish a completely 3D geometric information of terrain. This 3D information can be applied in many desciplines and now is an important data layer in GIS. The purpose of this research is to study the integrated procession of these two kinds of data. We have illustrated the mathematic models and algorithms for different processions respectively. From the results of procession, we can find out that raster-based extraction and display of terrain feature has better visualization and offers the alternative to processing.

REFERENCE

1. Lee, L. H., 1986, " A System Design for Digital Terrain Models and Applications in Automatic Topographic Mapping ", *J. of Survey Engineering*, Vol.28, #1, pp.9-24. (in Chinese)
2. Clarke, K. C., 1990, "Analytical and Computer Cartography ", Prentice-Hall, Englewood Cliffs, N. J., 290 pages.
3. Douglas, D. H., 1987, "Experiments to Locate Ridges and Channels to Create A new Type of Digital Elevation Model ", *The Canadian Surveyor*, Vol.41, No.3, pp.373-406.
4. Gillespie, A. R., Kahle, A. B., and Walker, R. E., 1986, " Color Enhancement of Highly Correlated Images ", *Remote Sensing of Environment*, Vol.20, pp.209-235.
5. Horn, B. K. P., 1981, " Hill Shading and Reflectance Map ", *Proceeding of IEEE*, Vol.69, No.1, pp.14-47.
6. Jenson, S. K. and Domingue, J. O., 1988, " Extracting Topographic Structure from Digital Elevation Data for Geographic Information System Analysis ", *Photogrammetric Engineering and Remote Sensing*, Vol.51, No.11, pp.1593-1600.
7. Junkin, B. G., 1982, " Development of Three-Dimensional Spatial Display Using A Geographically Based Information System ", *Photogrammetric Engineering and Remote Sensing*, Vol.48, No.4, pp.577-586.
8. Kennie, T. J. M., 1988, " Modelling for Digital Terrain and Landscape Visualisation ", *Photogrammetric Record*, 12(72), pp.711-745.
9. Kim, Y., 1989, " An IHS Color Model and Its Application ", *Proc. of American Society of Photogrammetry and Remote Sensing*, Vol.2, pp.43-52.
10. Lee, D. T., and Schachter, B. J., 1980, " Two Algorithm for Constructing a delaunay Triangulation ", *Internal Journal of Computer and Information Science*, Vol.9, No.3, pp.219-242.
11. McLaren R. A. and Kennie, T. J. M., 1988, " Computer Graphic Techniques for Generating Terrain and Landscape Visualisations ", *16th International Archives of Photogrammetry and Remote Sensing*, B3, Kyoto, pp.527-536.
12. Moik, J. G., 1980. " Digital Processing of Remote Sensed Image ", *U.S. Government Printing Office, Washington, D. C.*, 330 pages.
13. Monmonier, M. S., 1982, " Computer Assisted Cartography ", *Principles and Procspects*, Prentice-Hall, Englewood Cliffs, N. J., 214 pages.
14. Murai, S., 1985, " Digital Orthophoto Mapping Using A Digitized Aerial Photograph and Digital Terrain Model ", *Technique Report, Murai Laboratory, Institute of Industrial Science, Unkiversity of Tokyo.*
15. NCGIA, 1989, " Technical Issues in GIS-Lecute ", *University of California, Santa Barbara, USA.*
16. O'Callaghan, J. F., 1984, " The Extraction of Drainage Networks from Digital Elevation Data ", *Computer Vision, Graphics, and Image Processing* 28, pp.323-344.
17. Penna, M. A. and Patterson, P. R. 1986., " Projective Geometry and Its Application to Computer Graphics ", Prentice-Hall, Englewood Cliffs, N. J., 403 pages.
18. Yoeli, P., 1983, " Shadowed Contours With Computer and Plotter ", *The American Cartographer*, Vol.10, No.2, pp.101-110.